Available online at www.sciencedirect.com

ScienceDirect

Energy Procedia 55 (2014) 115 – 120

Energy Procedia

4th International Conference on Silicon Photovoltaics, SiliconPV 2014

Limitation of industrial phosphorus-diffused emitters by SRH recombination

Byungsul Min[a,*], Hannes Wagner[b], Amir Dastgheib-Shirazi[c], Pietro P. Altermatt[b]

[a]*Institute of Semiconductor Electronics, RWTH Aachen University, Sommerfeldstr. 24, 52074 Aachen, Germany*
[b]*Dep. Solar Energy, Inst. Solid-State Physics, Leibniz University of Hannover, Appelstr. 2, 30167 Hannover, Germany*
[c]*Department of Physics, University of Konstanz, Jacob-Burckhardt-Str. 29, 78464 Konstanz, Germany*

Abstract

It is commonly assumed in the PV community that Auger recombination is the dominant loss mechanism in heavily phosphorus-doped emitters of industrial Si solar cells. Contrary to this assumption, we show in this work that most of the losses are caused by Shockley-Read-Hall (SRH) recombination via defect states introduced by inactive phosphorus. Using numerical device simulations, we successfully reproduce all the measured J_{0e} values of a series of profiles (with various concentrations of inactive phosphorus) with an effective SRH capture crosses-section for holes, σ_p = 7.5×10^{-18} cm^2. The composition of inactive phosphorus (e.g. in form of clusters of interstitial phosphorus, fine and rod-shaped precipitates) may vary under different fabrication conditions, hence we do not claim that this σ_p value is globally valid. However, because the series of profiles is representative for many emitters in mass production, our result implies generally higher SRH than Auger recombination rates and has decisive implications on the improvement of such industrial emitters: many emitters have not yet reached the Auger-limit and they may still be significantly improved by reducing their density of inactive phosphorus.

© 2014 The Authors. Published by Elsevier Ltd. This is an open access article under the CC BY-NC-ND license
(http://creativecommons.org/licenses/by-nc-nd/3.0/).
Peer-review under responsibility of the scientific committee of the SiliconPV 2014 conference

Keywords: phosphorus precipitates; silicon solar cells; recombination; emitter

* Corresponding author. Tel.: +49-241-80-27892; fax: +49-241-80-22246.
E-mail address: min@iht.rwth-aachen.de

1876-6102 © 2014 The Authors. Published by Elsevier Ltd. This is an open access article under the CC BY-NC-ND license
(http://creativecommons.org/licenses/by-nc-nd/3.0/).
Peer-review under responsibility of the scientific committee of the SiliconPV 2014 conference
doi:10.1016/j.egypro.2014.08.090

1. Introduction

For most industrial crystalline Si solar cells, the low-cost screen-printed contacts require high phosphorus concentrations at the surface. Therefore, typical industrial diffusion processes result in profiles of electrically active phosphorus concentrations that are higher than 1×10^{20} cm^{-3} at the surface. Because of this high phosphorus surface concentration, it is widely accepted that Auger recombination is the dominant loss mechanism in such emitters. Based on this assumption it has been concluded that selective emitters suffer significantly less from recombination mainly because their peak dopant density is lowered.

On the other hand, it is well known that such heavily phosphorus-diffused emitters contain high amounts of electrically inactive phosphorus that may lead to precipitation phenomenons [1-4]. It was already suggested in the early 80s to consider these precipitates as SRH recombination centers, that influence the excess carrier lifetime in the emitter region and reduces the open-circuit voltage [5, 6].

Although recent progress demonstrates that the reduction of inactive phosphorus atoms improves cell efficiency considerably [7-9], it is not straight forward to determine whether SRH recombination (due to inactive phosphorus) is stronger than is Auger recombination (caused by the active phosphorus atoms).

To answer conclusively this question we analyse various emitter profiles, published in Ref. [10], where the amount of active and inactive phosphorus atoms was varied. In order to account for the influence of inactive phosphorus in our device simulation, we interpret it by SRH recombination as indicated in Ref. [6]. The fact that all measured saturation current density J_{0e} values of the series of profiles can be successfully reproduced strongly indicates that the SRH recombination is the dominant loss mechanism in heavily doped emitters of typical industrial Si solar cells.

2. Simulation model

The numerical device simulations are performed with the software SENTAURUS in two dimensions. We apply the most recent silicon material parameters and device models from Ref. [11] and include the recently published parameterization for Auger recombination of Richter et al. [12]. Fig. 1 shows two representative density profiles of the active phosphorus N_{don}, obtained from electrochemical capacitance-voltage (ECV) measurements, and of the total phosphorus N_P, from secondary ion mass spectroscopy (SIMS) measurements [10]. Near the surface, we correct the SIMS profiles with the dotted red line to eliminate measurement artefacts.

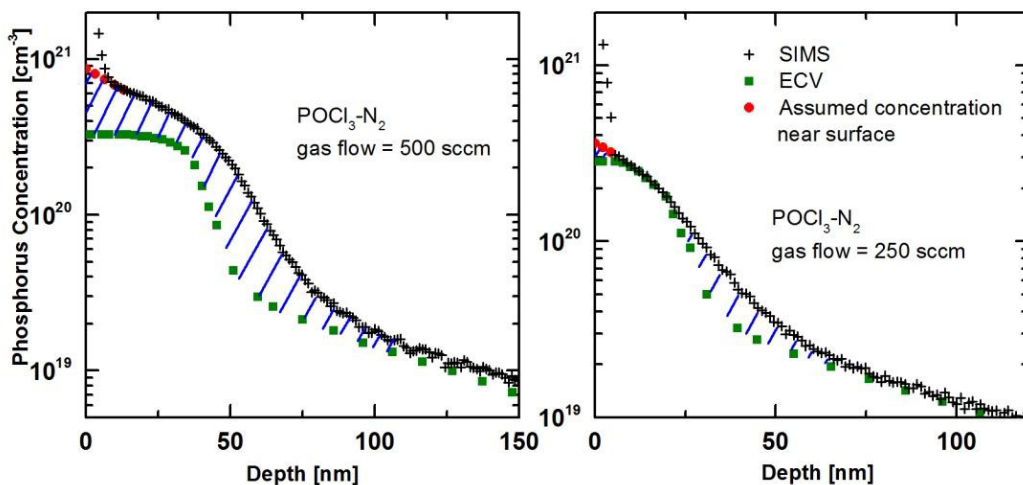

Fig. 1. Two representative SIMS and ECV measurements of $POCl_3$ emitters from Ref. [10]. The hashed area indicates the density of inactive phosphorus.

The difference between N_P and N_{don} is shown as hashed area and indicates the concentration of inactive phosphorus N_i. It can be either in form of interstitial P atoms, inactive P clusters, fine silicon phosphide (SiP) precipitates, or even rod-like SiP structures. Since we do not know the exact composition, we choose N_i as effective density of a single type of defect, thus the SRH capture cross-section for holes, σ_p, has an effective meaning. Note that, at low $POCl_3$ flows, the amount of N_i is very small, while at high $POCl_3$ flows, there is a spill-over of precipitates up to 140 nm deep, where N_{don} drops down to 2×10^{19} cm^{-3}. Accordingly, the high minority carrier concentration in that region results in high SRH recombination rates. The starting material of the analysed experiment consists of boron-doped float zone wafers with a specific resistivity of 200 Ωcm. To measure the saturation current density J_{0e} values, the emitters on both wafer surfaces were passivated using plasma enhanced chemical vapour deposition and were fired in a conveyor belt furnace to facilitate hydrogen passivation. See Ref. [10] for a detailed description of the experiment.

3. Results and discussion

The measured J_{0e} values of all profiles in Ref. [10] can be reproduced in these simulations by *concurrently* adjusting a single value of σ_p for all profiles, and by keeping the SRH surface recombination velocity of minority carriers S_p as a free parameter. In order to distinguish which recombination type dominates, we consider the following two scenarios: (i) the "Auger scenario" neglects SRH recombination via inactive phosphorus, thus Auger recombination dominates; (ii) the "SRH scenario" takes SRH recombination via inactive phosphorus additionally into account. In both cases, SRH surface recombination and SRH bulk recombination (via the usual defects in the wafer) as well as radiative recombination are taken into account.

Fig. 2(a) compares the measured with the simulated J_{0e} values in dependence of the $POCl_3$-flow maintained during deposition of the phosphorus silicate glass (PSG) layer. Because the SRH surface recombination velocity of minority carriers S_p is a free parameter, it is plotted in Fig. 2(b) in dependence of the total phosphorus concentration N_P at the surface, $N_{P,surf}$. The measured J_{0e} values (crosses) can be reproduced with the Auger scenario (circles) only for very low $POCl_3$ flows, even if setting S_p to its physical limit, the thermal velocity v_{th}. By contrast, the SRH scenario reproduces all measured J_{0e} values (open rectangles) if using $\sigma_p = 7.5\times10^{-18}$ cm^2. Additionally, we observed in the SRH scenario that (i) for $\sigma_p < 7.5\times10^{-18}$ cm^2, the simulation cannot reproduce all of the measured J_{0e} values, even when setting $S_p = v_{th}$; (ii) for $\sigma_p > 9\times10^{-18}$ cm^2, the simulation overestimates J_{0e} of some samples in Ref. [10];

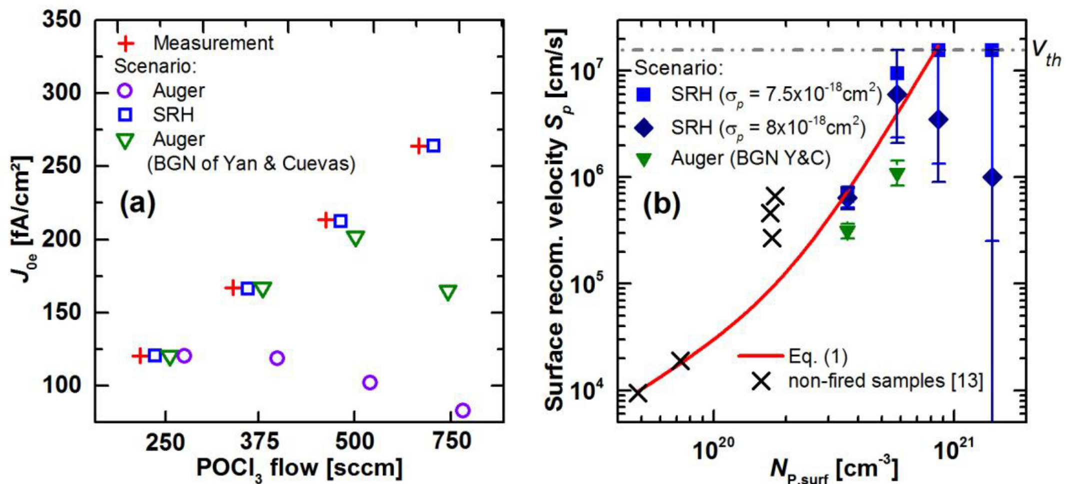

Fig. 2. Left: comparison of J_{0e} measurement (crosses) of the samples in Ref. [10] at an injection density of 5×10^{15}cm^{-3} with our simulated J_{0e} values using three different scenarios. Right: the resulting S_p in dependence of $N_{P,surf}$. The line indicates an empirical parameterisation of S_p. Literature data of non-fired samples are shown for comparison (crosses)[13]. The error bars are determined by assuming 10% uncertainty in the J_{0e} measurements.

(iii) even by using σ_p = 8×10^{-18} cm^2, the resulting S_p values (diamonds) decrease towards high $N_{P,surf}$ in Fig. 2(b), which does not make physically sense. Hence, only a very narrow range near σ_p = 7.5×10^{-18} cm^2 eliminates any inconsistency between simulations and these experiments.

One possible empirical parameterisation of S_p, shown as line in Fig. 2(b), is:

$$S_p = 1091\frac{\text{cm}}{\text{s}} \cdot \left(\frac{N_{\text{P,surf}}}{10^{19}\,\text{cm}^{-3}}\right)^{1.37} + 0.6\frac{\text{cm}}{\text{s}} \cdot \left(\frac{N_{\text{P,surf}}}{10^{19}\,\text{cm}^{-3}}\right)^{3.84} \quad (1)$$

for $N_{P,surf}$ up to 8.4×10^{20} cm^{-3} for fired SiN_x layers.

Alternative to this explanation, Yan and Cuevas [14] recently fabricated a series of emitters and reproduced their measured J_{0e} values by empirically adjusting band gap narrowing (BGN). Indeed, they obtained a consistent BGN model, which yields a significantly stronger gap-shrinkage than Schenk's quantum-mechanical model [15], which is used in our simulations. We therefore tried to reproduce the J_{0e} values of Fig. 2(a) by using Yan and Cuevas' BGN model. While such simulations (open triangles) reproduce J_{0e} significantly better than with our Auger scenario, the model is unable to reproduce J_{0e} at the $POCl_3$ flows of 500 and 750 sccm, even if setting $S_p = v_{th}$. With the BGN model of Yan and Cuevas, we simulated other emitters from industry, but failed in many cases. Our simulations of ion-implanted emitters, where no precipitates are present, significantly overestimate J_{0e} when using that BGN model.

At high dopant densities, however, the Schenk's BGN model may underestimate the gap-shrinkage, since the model does not account the increase of electron masses shown in Fig. 3(a). In order to clarify this uncertainty, we revised the Schenk's BGN model by considering the increase of electron masses. Therefore, we perform an empirical parameterization of measured data in Fig. 3(a), we then use this parameterization as multiplication factor for the reduced effective mass in Schenk's Padé approximation by assuming that the hole masses stay constant as observed in Ref. [16, 17]. As result, we found only a slight increase in BGN is derived compared to Schenk's original BGN as shown as red dashed line in Fig. 3(b). We found currently no other physical reason why BGN should be as strong as proposed by Yan and Cuevas.

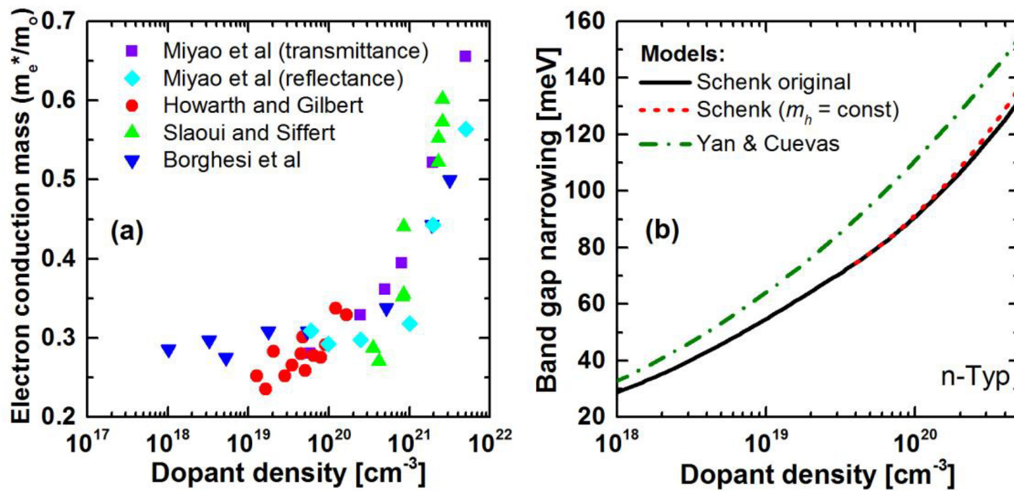

Fig. 3. Left: electron conduction mass in n-type silicon, measured by reflection [18-21] and by transmission [19]. Right: comparison of different BGN models

4. Implication

These findings have very useful implications to the fabrication of typical industrial emitters: A) their recombination losses are still dominated by SRH recombination and not Auger recombination; B) because inactive phosphorus may exist in various forms in various proportions of phosphorus clusters and precipitates, there will be no universal emitter model available for optimisation, but must be tuned to fabrication conditions. C) The good news is that this gives manipulation opportunities to significantly improve emitters by reducing the density of inactive phosphorus, e.g. by tuning the $POCl_3$-flow, by solid-state diffusion, or epitaxy. This finding is also predicted by process and device simulations using SENTAURUS shown in Fig. 4 and described in details in a forthcoming paper – while Yan and Cuevas imply that there is no perspective for improvement except by reducing N_{dop}.

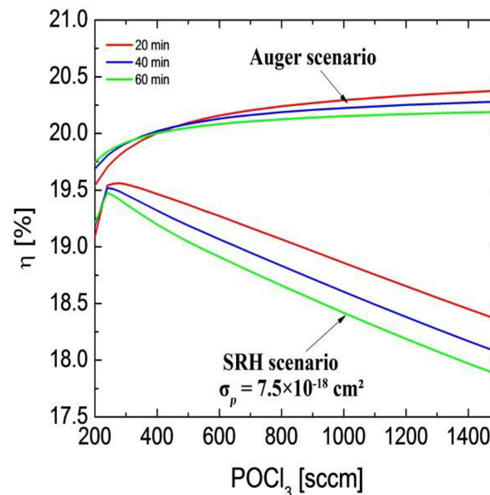

Fig. 4. Process and device simulations of industrial-type PERC cells predict that avoiding inactive phosphorus in the homogeneous emitter may increase cell efficiency by about 0.5% absolute.

5. Conclusion

In this paper, we show that the SRH recombination caused by inactive phosphorus dominates the recombination process in a typical series of heavily doped emitters of industrial Si solar cells. For modelling the influence of inactive phosphorus, we suggest to interpret it by SRH recombination with capture cross section for holes around 7.5×10^{-18} cm^2.

As alternative to our suggestion, the empirical BGN model of Yan and Cuevas can be applied for modelling heavily doped emitters. However, this model may not be suitable to describe carrier recombination in samples with high amount of inactive phosphorus atoms, if the SRH recombination due to inactive phosphorus is not accounted.

These results imply opportunities for significant improvement of cell efficiency by reducing the density of inactive phosphorus atoms, as demonstrated in Ref. [7-9].

Acknowledgements

The authors thank Andreas Schenk for fruitful discussions and his support by revision of BGN model. This work is a part of the project “NIL-TEX” and has been supported by the European Union European Regional Development Fund and by the Ministry of Economic Affairs and Energy of the State of North Rhine-Westphalia, Germany.

References

[1] E. Tannenbaum. Detailed analysis of thin phosphorus-diffused layers in p-type silicon. Solid-State Electronics 1961; 2: 123-132.
[2] A. Armigliato et al. SiP precipitation within the doped silicon lattice, concomitant with phosphorus predeposition. J. Appl. Phys. 1976; 47: 5489-5491.
[3] D. Nobili et al. Precipitation as the phenomenon responsible for the electrically inactive phosphorus in silicon. J. Appl. Phys. 1982; 53: 1484-1491.
[4] S. Solmi et al. Dopant and carrier concentration in Si in equilibrium with monoclinic SiP precipitates. Physical review. B, Condensed matter 1996; 53: 7836-7841.
[5] D. Nobili. Solid Solubility and Precipitation of Phosphorus and Arsenic in Silicon Solar Cells Front Layer. in Proc. of the Fourth E.C. Photovoltaic Solar Energy Conference, 1982, p. 410-420.
[6] P. Ostoja et al. The effects of phosphorus precipitation on the open-circuit voltage in N+/P silicon solar cells. Solar Cells 1984; 11: 1-12.
[7] Y. Komatsu et al. Innovative diffusion processes for improved efficiency on industrial solar cells by doping profile manipulation. in Proc. of the Proceedings of the 24th European Photovoltaic Solar Energy Conference and Exhibition, 2009, p. 1063-1067.
[8] J. Horzel et al. Homogeneous Versus Selective Emitters - Perspectives for Future Industrial Processing of Crystalline Silicon Solar Cells. in Proc. of the Proceedings of the 25th European Photovoltaic Solar Energy Conference, 2010, p. 1492-1498.
[9] A. Dastgheib-Shirazi et al. Towards an optimized emitter for screen-printed solar cells. in Proc. of the 39th IEEE Photovoltaic Specialists Conference, Tempa, Florida, 2013.
[10] A. Dastgheib-Shirazi et al. Relationships between Diffusion Parameters and Phosphorus Precipitation during the POCl3 Diffusion Process. Energy Procedia 2013; 38: 254-262.
[11] P.P. Altermatt. Models for numerical device simulations of crystalline silicon solar cells—a review. Journal of computational electronics 2011; 10: 314-330.
[12] A. Richter et al. Improved quantitative description of Auger recombination in crystalline silicon. Physical Review B 2012; 86: 165202.
[13] P.P. Altermatt et al. Numerical modeling of highly doped Si:P emitters based on Fermi--Dirac statistics and self-consistent material parameters. J. Appl. Phys. 2002; 92: 3187-3197.
[14] D. Yan, A. Cuevas. Empirical determination of the energy band gap narrowing in highly doped n+ silicon. J. Appl. Phys. 2013; 114: 044508.
[15] A. Schenk. Finite-temperature full random-phase approximation model of band gap narrowing for silicon device simulation. J. Appl. Phys. 1998; 84: 3684-3695.
[16] E. Barta. Determination of effective mass values by a Kramers-Kronig analysis for variously doped silicon crystals. Infrared Physics 1977; 17: 111-119.
[17] A. Borghesi et al. Fundamental optical properties of heavily-boron-doped silicon. Physical Review B 1987; 36: 9563-9568.
[18] L.E. Howarth, J.F. Gilbert. Determination of Free Electron Effective Mass of n-Type Silicon. J. Appl. Phys. 1963; 34: 236-237.
[19] M. Miyao et al. Change of the electron effective mass in extremely heavily doped n-type Si obtained by ion implantation and laser annealing. Solid State Commun. 1981; 37: 605-608.
[20] A. Slaoui, P. Siffert. Determination of the Electron Effective Mass and Relaxation Time in Heavily Doped Silicon. Phys. Status Solidi A 1985; 89: 617-622.
[21] A. Borghesi et al. Optical determination of Si conduction-band nonparabolicity. J. Appl. Phys. 1990; 67: 3102-3106.